IJAE
Vol. 120, n. 3: 184-191, 2015
ITALIAN JOURNAL OF ANATOMY AND EMBRYOLOGY

Research Article – Basic and applied anatomy

3D reconstruction and heat map of porcine recurrent laryngeal nerve anatomy: branching and spatial location

Nena Lundgreen Mason[1,*], Marc Christiansen[1], Jonathan J. Wisco, Ph.D.[1,2]

[1]Department of Physiology and Developmental Biology, Neuroscience Center, Brigham Young University, Provo, UT, and [2]Department of Neurobiology and Anatomy, University of Utah Medical School, Salt Lake City, UT

Submitted May 21, 2015; accepted August 4, 2015

Abstract

Recurrent laryngeal nerve palsy is a common post-operative complication of many head and neck surgeries. Theoretically, the best treatment to restore partial function to a damaged recurrent laryngeal nerve would be reinnervation of the posterior cricoarytenoid muscle via anastomosis of the recurrent laryngeal and phrenic nerves. The pig is an excellent model of human laryngeal anatomy and physiology but a more thorough knowledge of porcine laryngeal anatomy is necessary before the pig can be used to improve existing surgical strategies, and develop new ones. This study first identifies the three most common recurrent laryngeal nerve branching patterns in the pig. Secondly, this study presents three-dimensional renderings of the porcine larynx onto which the recurrent laryngeal nerve patterns are accurately mapped. Lastly, heat maps are presented to display the spatial variability of recurrent laryngeal nerve trunks and primary branches on each side of 15 subjects (28 specimens). We intend for this study to be useful to groups using a porcine model to study posterior cricoarytenoid muscle reinnervation techniques.

Key words

Porcine larynx, recurrent laryngeal nerve, larynx model

Introduction

Vocal cord paralysis is a common post-operative complication of head and neck procedures that is caused by damage to the recurrent laryngeal nerve (RLN) (Li et al., 2013). Vocal cord paralysis can cause respiratory compromise if innervation to the posterior cricoarytenoid muscle (PCA) is compromised. PCA dysfunction renders the vocal folds unable to abduct, yielding respiratory compromise. In theory, the most effective way to correct this problem would be to selectively reinnervate the PCA (Li et al., 2013). Reinnervation of the PCA has been achieved via anastomosis of the RLN with the phrenic nerve in both human and animal models (Crumley, 1983; Jacobs et al., 1990; Sanders et al., 1993; van Lith-Bijl et al., 1998). The phrenic nerve is the best choice for anastomosis with the RLN because the two nerves are compatible in histological, electrophysiological, and anatomical parameters (Crumley, 1983; Jacobs et al., 1990; Sanders et al., 1993; van Lith-Bijl et al., 1998). In theory, phrenic/RLN anasto-

* Corresponding author. E-mail: nenalundgreen@gmail.com

http://www.fupress.com/ijae
DOI: 10.13128/IJAE-17815

mosis would be the best treatment for vocal cord paralysis (Li et al., 2013) but current methods are not consistently successful. Improvements need to be made to this surgical technique to increase its effectiveness.

Animal models have long been used to develop and improve surgical strategies for use on human patients. Animal model selection for surgical development is generally dependent on how analogous a particular animal is to human anatomy. The pig larynx is the most similar to that of humans in its anatomy (Gorti et al., 1999), neuroanatomy (Stavroulaki and Birchall, 2001), mucosal histology (Gorti et al., 1999), and phonatory characteristics (Jiang et al., 2001; Knight et al., 2005) among the various animal models that have been used in past studies. Due to these similarities between human and porcine laryngeal anatomy the pig is the ideal choice for the development and improvement of PCA reinnervation surgical procedures. As with any surgery a detailed understanding of the anatomy and possible anatomical variations is necessary so that effective pre-clinical studies can be developed using the porcine model.

Traditional anatomy atlases contain detailed 2D drawings of body structures. A two dimensional atlas does not include vital information that well planned surgery requires such as the depth of a particular structure, its precise distance from surrounding structures, and the spatial relationships between different tissues. 3D anatomical representations of body structures reflect true anatomical arrangement and eliminate the risk of misrepresentation of 3D structures that is common amongst 2D diagrams. Currently this type of spatial information is available through dissection experience, exploratory surgery and a few imaging techniques. Various techniques exist to obtain images of anatomical structures that are accurate in three dimensions, such as volume rendering (Coll et al., 2000; Lawler and Fishman, 2001), but these techniques require expensive computerized tomography equipment and are only available to researchers with access to medical facilities. Surgical planning, anatomical education and preclinical research would greatly benefit from easy access to accurate 3D representations of anatomical structures.

In this study we present data-driven 3D models of the porcine RLN to be used for anatomical education and for planning surgical experiments of PCA reinnervation. Each nerve is shown in accurate relation to surrounding laryngeal structures including the thyroid and arytenoid cartilages, PCA, epiglottis, and trachea. This study is intended to be useful to research groups using the pig to improve and further develop PCA surgical reinnervation strategies.

Materials and Methods

Animals

Fifteen porcine larynges used in this study were donated by Circle V Meats (Spanish Fork, Utah). From the 15 larynges 28 RLNs were undamaged during the excision process and were used in the study. Larynx specimens were opportunity samples obtained from animals that were sacrificed for commercial purposes over the course of one month. Excess tissue was removed from each specimen leaving only cartilage, trachea, esophagus, laryngeal nerves, and intrinsic muscles of the larynx. A 10% formalin solution was used to fix and preserve the larynges for storage prior to dissection.

Dissection of the porcine recurrent laryngeal nerve

Great care was given during dissection to maintain the structural integrity of each RLN in all specimens. The RLN trunk was identified in the tracheoesophageal groove just inferior to the level of the cricoid cartilage. Careful dissection techniques were used to prevent displacement of RLNs from surrounding fascia and tissue. The RLN trunk was followed superiorly using blunt dissection until primary branching began.

From the point of primary branching through individual branch termination a more delicate visually controlled method was used to clearly expose the unique branching pattern of each nerve specimen. The superficial surface of the primary and secondary nerve branches were exposed distally while leaving the lateral and deep aspects of the nerve imbedded in fascia. For each dissected nerve specimen, the branching pattern was photographed, drawn, and digitized with a MicroScribe G apparatus (GoMeasure3D, Amherst, VA) for subsequent categorical analysis and modeling.

MicroScribe 3D digitization

Each RLN trunk was digitized in 1 mm increments starting at the level of the posterior inferior border of the thyroid cartilage, then proceeding distally through primary and secondary (where possible) branching. The medial and inferior borders of the ipsilateral thyroid cartilage, epiglottis, and the line of cricoid cartilage visible at the midline of the PCA were also digitized along with each nerve specimen to insure accurate spatial placement of RLNs during the generation of 3D models. The data points acquired from RLN digitization were imported into Maya (Autodesk, San Rafael, CA) and used to create a 3D rendering of each nerve specimen.

Heat map

We captured a posterolateral *en face* view of each RLN rendering from the same angle and imported the image into Photoshop CC (Adobe Systems, San Jose, CA). Each digitized thyroid cartilage and epiglottis with its accompanying RLN reconstruction was linearly scaled to a reference 3D reconstruction, resulting in an anatomically comparable spatial composite of all 28 specimens. The RLNs were masked in each of the layers of the composite, and converted to grayscale at 50 % opacity. Then the composite was flattened and pseudo-colored to generate a heat map that qualitatively shows the likelihood of finding an RLN branch in a given location (Wisco et al., 2012). We also created a composite of registered RLN trunks to depict variation in mediolateral trunk location.

Results

Porcine recurrent laryngeal nerve anatomical variations

We identified three common RLN branching patterns in the pig. Primary branching varied in location of bifurcation from the RLN trunk and in the total number of

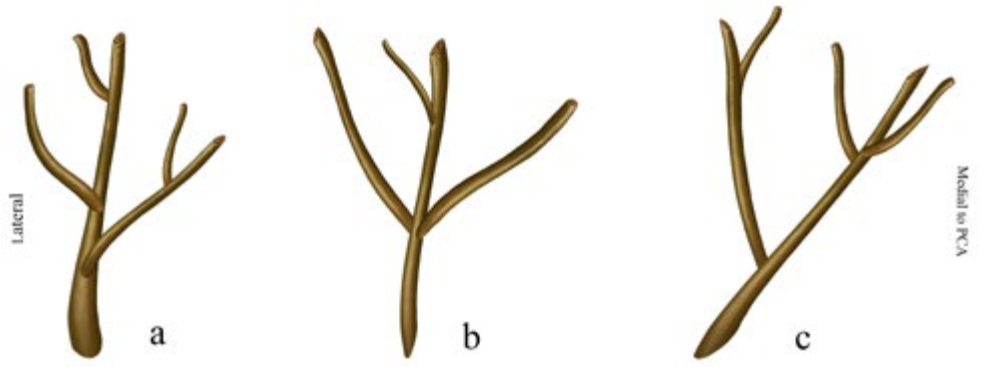

Figure 1 – The three prevailing branching patters of the porcine recurrent laryngeal nerve. 25 specimens were dissected and analyzed. A. The most common variation of the RLN was found in 44% of observed larynges. B. The second most common RLN branching pattern was found in 32% of larynges. C. The least common RLN branching pattern was found in 24% of larynges.

branches. The lateral secondary RLN branch innervated the interarytenoid, thyroarytenoid, and lateral cricoarytenoid muscles in various terminal distributions to facilitate vocal fold adduction. Innervation of the PCA muscle was conserved among all specimens via projections of the medial primary branch of the RLN trunk but we also observed substantial distal variation in branching before branch termination into the muscles of the larynx. Figure 1 exhibits the three main variations of primary RLN branching in the pig.

Our data suggests that of the three primary porcine branching patterns, A is the most common, being found in 44% of larynges dissected. Specimens exhibiting branching pattern A all possessed the following attributes; the most proximal branch to diverge from the RLN trunk was a medial primary branch which bifurcated into two secondary branches both of which clearly went on to innervate the PCA muscle. The second branch to arise from the RLN trunk was a lateral primary branch that split into various small terminal branches all of which ran away from the PCA to innervate the laryngeal adductor muscles. Distal to the lateral primary branch there was the middle primary branch which also innervated the intrinsic laryngeal adductor muscles.

The second most common pattern, B, in which three primary branches (medial, middle, and lateral) arose from the RLN trunk simultaneously, occurred in 32% of our specimens. In all specimens of pattern B, the medial primary branch innervated the PCA along with half of the terminal branches of the middle primary branch. The other half of the terminal branches of the middle primary branch ran away from the PCA and targeted adductors along with the lateral primary branch.

Pattern C was found in 24% of our larynx specimens. RLNs that exhibited branching pattern C possessed two primary branches, one medial and one lateral arising from the RLN trunk concurrently. The medial of these two branches further diverged into a superior, middle, and inferior secondary branches as it projected toward the

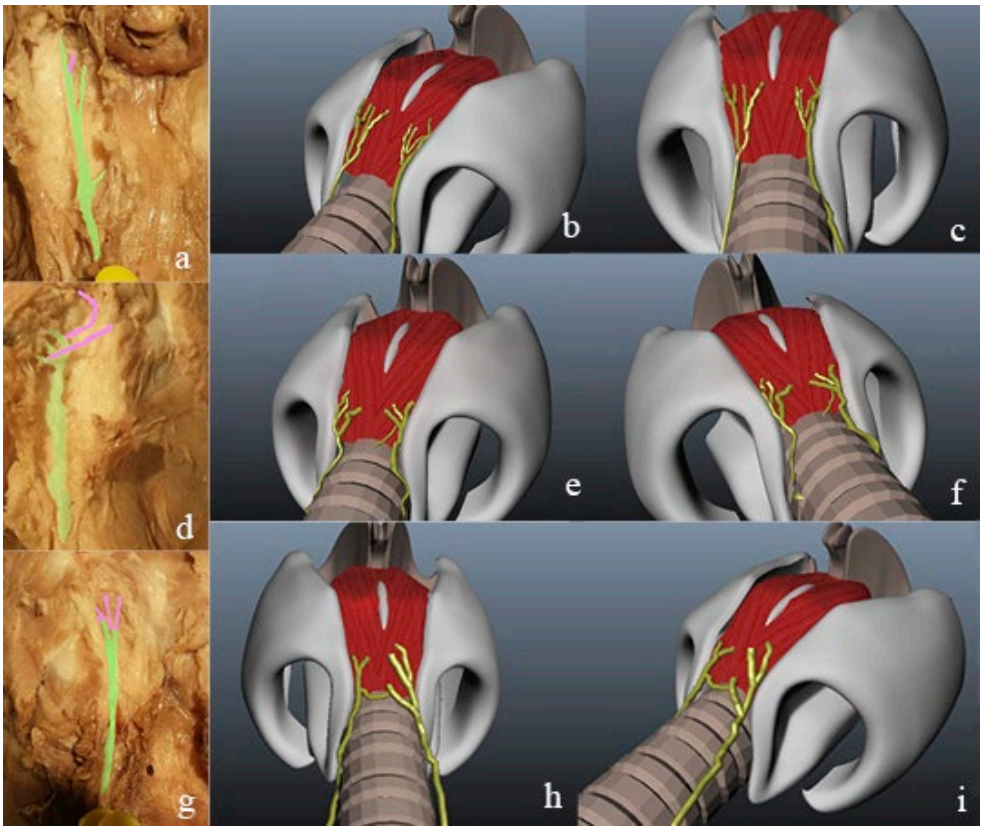

Figure 2 – Images of cadaveric porcine larynx specimens that are representative of the three major RLN branching patterns. Cadaveric images are accompanied by 3D renderings showing precise RLN placement in relation to other structures within the larynx. The nerve has been highlighted for clear viewing, with the RLN trunk and primary branching shown in green and secondary branches shown in purple. a-c: Images of branching pattern A, the most common porcine branching pattern. c-d: Images of branching pattern B, the second most common pattern. g-i: Images of branching pattern C, the least common pattern.

PCA. The most superior of these secondary branches appeared to run supero-laterally and possibly innervated vocal fold adductors, whereas the middle and inferior secondary branches clearly innervated the PCA.

3D laryngeal representation

The MicroScribe data for each nerve and reference structure was imported into Maya and rendered into a 3D model. After each of the RLN specimens was carefully fit onto an individual larynx scaffold rendering, three bilateral larynges were selected for inclusion in Figure 2. Each of the three larynges selected represent one of the three major RLN primary branching patterns found in the pig. Figure 2 illustrates the

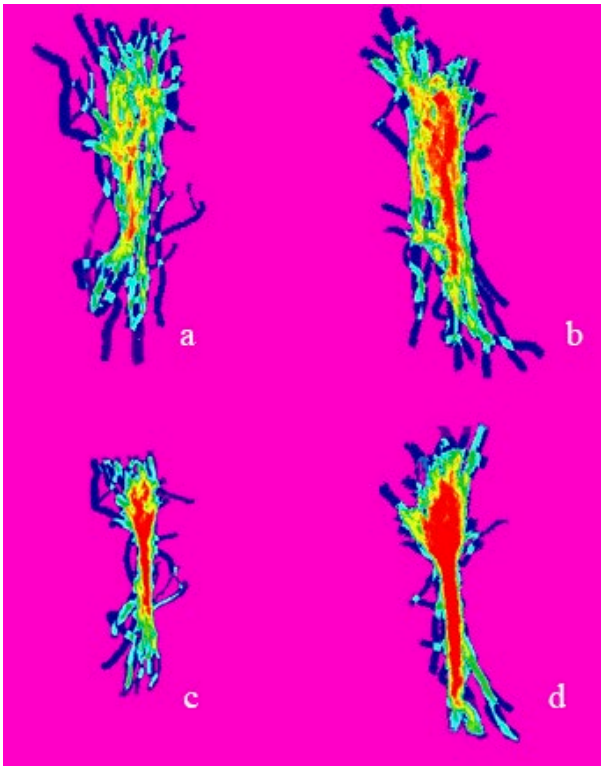

Figure 3 – A heat map depicting the relative spatial variability from one RLN specimen to the next; n=28. The left column represents left nerve specimens and the right column represents the right nerve specimens. a, b: Relative spatial location of the left and right RLNs respectively. c, d: Comparison of RLN primary branching patterns amongst left and right RLNs respectively after the trunks were registered together by the RLN trunk and its primary branching point.

best dissection of a specimen for each of the three patterns, and a representative 3D model of the same branching pattern. Each row of the figure accurately shows where the recurrent laryngeal nerve sits within the larynx. Renderings of all of our specimens can be viewed through The National Repository for Laryngeal Data which can be freely accessed at www.nrld.org.

Heat maps

Figures 3a and 3b depict the relative spatial location of each RLN within the larynx and represent the probability of finding the RLN in a given area. Our data show that the RLN on the right side of the larynx has a more consistent and predictable medial/lateral RLN trunk location as indicated by the solid red areas (Figure 3b). The RLN on the left side of the larynx displays higher variability in RLN trunk and branch location (Figure 3a).

Figure 3c and 3d depict the RLN and its branching pattern after the RLN trunks were linearly registered.

Discussion

Our data suggest that the medial/lateral position of the nerve is more consistent on the right than the left side of the larynx (Figure 3a and 3b). This information is important for two reasons. First, the variability of left RLN location could make it more vulnerable to accidental transection during head and neck surgery. If the human larynx were to possess a similar dichotomy between the right and left RLN, this would need to be included in surgical planning to avoid accidental damage.

Second, this finding is also relevant when considering phrenic/RLN anastomosis for PCA reinnervation surgery. Because the variability of nerve position is greater on the left it could be more difficult to use left RLNs in PCA reinnervation via phrenic nerve anastomosis. It has been shown that the left phrenic nerve is the best choice to use in an RLN anastomosis procedure (Li et al 2013). Our data suggest that the right RLN is an easier choice for anastomosis in porcine experimental surgery because its position is more consistent. Unfortunately the right RLN, which is more consistently located, is contralateral to the left phrenic nerve.

However, we also showed spatial variations in the primary branching pattern of the porcine RLN (Figure 3c and 3d). It is interesting to note that although the right RLN as a whole is more consistently found in the same place, the primary branches of right RLNs exhibit much more variation in location. In contrast, the branches on the left RLNs are quite congruent. Not only are they consistent in location, they are often found to display the same anatomical branching pattern.

The images and models of porcine laryngeal anatomy presented in this study were created to be useful to those studying PCA reinnervation techniques in a porcine model. Our images and models could also be used in an educational setting to easily illustrate accurate 3D relationships between laryngeal structures. Observations made from our heat maps regarding discrepancies in right/left structural location of the recurrent laryngeal nerve also raise interesting questions that should be examined in the human larynx. If the human larynx were to possess a similar dichotomy between the right and left RLN, this would need to be included in surgical planning to avoid accidental damage.

Acknowledgements

The authors would like to acknowledge Circle V Meats (Spanish Fork, Utah) for their generosity in providing the porcine larynx specimens for this study. We thank Mr. Ryan McAdam for his assistance rendering the digital larynx model and Mr. Sean Higgins for his assistance with the nerve diagrams in our figures. This study was funded by the Brigham Young University, College of Life Sciences, Start-Up Mentoring Environment Grant and NIH/NIDCD 5R01DC009616-05.

References

Coll D.M., Herts B.R., Davros W.J., Uzzo R.G., Novick A.C. (2000) Preoperative use of 3D volume rendering to demonstrate renal tumors and renal anatomy 1. Radiographics 20: 431-438.

Crumley R. (1983) Phrenic nerve graft for bilateral vocal cord paralysis. Laryngoscope 93: 425-428.

Gorti G.K., Birchall M.A., Haverson K., Macchiarini P., Bailey M. (1999) A preclinical model for laryngeal transplantation: anatomy and mucosal immunology of the porcine larynx. Transplantation 68: 1638-1642.

Jacobs I., Sanders I., Wu B., Biller H. (1990) Reinnervation of the canine posterior cricoarytenoid muscle with sympathetic preganglionic neurons. Ann. Otol. Rhinol. Laryngol. 99: 167-174.

Jiang J.J., Raviv J.R., Hanson D.G. (2001) Comparison of the phonation-related structures among pig, dog, white-tailed deer, and human larynges. Ann. Otol. Rhinolo. Laryngol. 110: 1120-1125.

Knight M.J., McDonald S.E., Birchall M.A. (2005) Intrinsic muscles and distribution of the recurrent laryngeal nerve in the pig larynx. Eur. Arch. Otorhinolaryngol. 262: 281-285.

Lawler L.P., Fishman E.K. (2001) Multi–detector row CT of thoracic disease with emphasis on 3D volume rendering and CT angiography 1. Radiographics 21: 1257-1273.

Li M., Chen S., Zheng H., Chen D., Zhu M., Zhu M., Wang W., Liu F., Zhang C. (2013) Reinnervation of bilateral posterior cricoarytenoid muscles using the left phrenic nerve in patients with bilateral vocal fold paralysis. PloS One 8: e77233.

Sanders I., Wu B.-L., Mu L., Li Y., Biller H.F. (1993) The innervation of the human larynx. Arch. Otolaryngol. Head Neck Surg. 119: 934-939.

Stavroulaki P., Birchall M. (2001) Comparative study of the laryngeal innervation in humans and animals employed in laryngeal transplantation research. J. Laryngol. Otol. 115: 257-266.

van Lith-Bijl J.T., Stolk R.J., Tonnaer J.A., Groenhout C., Konings P.N., Mahieu H.F. (1998) Laryngeal abductor reinnervation with a phrenic nerve transfer after a 9-month delay. Arch. Otolaryngol, Head Neck Surg. 124: 393-398.

Wisco J.J., Stark M.E., Safir I., Rahman S. (2012) A heat map of superior cervical ganglion location relative to the common carotid artery bifurcation. Anesth. Analg. 114: 462-465.